Fgf signaling instructs position-dependent growth rate during zebrafish fin regeneration

Yoonsung Lee[1], Sara Grill[1], Angela Sanchez[2], Maureen Murphy-Ryan[1] and Kenneth D. Poss[1,*]

[1]Department of Cell Biology, Duke University Medical Center, Durham, NC 27710, USA
[2]Department of Cardiology, Children's Hospital, Boston, MA 02115, USA
*Author for correspondence (e-mail: k.poss@cellbio.duke.edu)

Accepted 22 September 2005

Development 132, 5173-5183
Published by The Company of Biologists 2005
doi:10.1242/dev.02101

Summary

During appendage regeneration in urodeles and teleosts, tissue replacement is precisely regulated such that only the appropriate structures are recovered, a phenomenon referred to as positional memory. It is believed that there exists, or is quickly established after amputation, a dynamic gradient of positional information along the proximodistal (PD) axis of the appendage that assigns region-specific instructions to injured tissue. These instructions specify the amount of tissue to regenerate, as well as the rate at which regenerative growth is to occur. A striking theme among many species is that the rate of regeneration is more rapid in proximally amputated appendages compared with distal amputations. However, the underlying molecular regulation is unclear. Here, we identify position-dependent differences in the rate of growth during zebrafish caudal fin regeneration. These growth rates correlate with position-dependent differences in blastemal length, mitotic index and expression of the Fgf target genes *mkp3*, *sef* and *spry4*. To address whether PD differences in amounts of Fgf signaling are responsible for position-dependent blastemal function, we have generated transgenic fish in which Fgf receptor activity can be experimentally manipulated. We find that the level of Fgf signaling exhibits strict control over target gene expression, blastemal proliferation and regenerative growth rate. Our results demonstrate that Fgf signaling defines position-dependent blastemal properties and growth rates for the regenerating zebrafish appendage.

Key words: Zebrafish, Fin, Regeneration, Blastema, Fibroblast growth factor

Introduction

Adult teleost fish and urodele amphibians can regenerate entire amputated appendages. In striking contrast, regenerative healing of mammalian limbs is limited to the very tips of digits. Although appendage regeneration has been studied for over three centuries, many mysteries remain. Understanding the cellular and molecular mechanisms by which lower vertebrate model systems are able to faithfully regenerate complex organs will help illuminate potential therapies for diseases of organ damage in humans.

One of the most striking features of appendage regeneration is the recognition and replacement of only those structures removed by amputation. This phenomenon, often called positional memory, has been studied most in the regenerating newt or axolotl limb. During limb regeneration, developmental regulation of regenerative growth rate is a prominent component of positional memory. For example, when a salamander is given an upper arm amputation on one limb and a digit level amputation on the other, regeneration of both limbs is completed in approximately the same time period (Spallanzani, 1769). Thus, the greater amount of tissue that is amputated, the faster is the rate of regeneration. This phenomenon has been observed in many other lower vertebrate species, including teleosts goldfish, killifish and gourami, and in invertebrates such as starfish (Morgan, 1906; Tassava and Goss, 1966). The evolutionary persistence of position-dependent growth rate suggests a fundamental role for this regulatory mechanism in the process of regeneration.

Studies from the past several decades have attempted to identify morphological factors that distinguish proximal regenerates (the more proximal amputation level) from distal regenerates (the more distal amputation level). For example, although proximal regenerates with high growth rate usually have greater stump dimensions after amputation, Tassava and Goss (Tassava and Goss, 1966) found that stump diameter showed no consistent correlation with rates of lizard tail regeneration. Furthermore, young salamanders with smaller limbs can regenerate considerably faster than older animals with large limbs (Goodwin, 1946). In other studies, Maden (Maden, 1976) found no differences in volume or proliferation characteristics between the proximal and distal axolotl limb blastema, the so-called mass of undifferentiated mesenchymal tissue that ultimately gives rise to new structures. Similarly, Iten and Bryant (Iten and Bryant, 1973) did not detect growth rate differences in initial formation of the salamander limb blastema, but instead saw the greatest difference in growth rates during later morphogenesis and differentiation phases. Although morphological studies have pointed out useful correlations between anatomy and growth rate, there has been

very little molecular definition of the underlying regulation responsible for position-specific regenerative properties.

Over the past several years, the zebrafish, which regenerates fins (Johnson and Weston, 1995), spinal cord tissue (Becker et al., 2004) and heart muscle (Poss et al., 2002a; Raya et al., 2003), has gained popularity as a model for teleost appendage regeneration. Indeed, molecular genetic analysis in zebrafish has a unique potential to facilitate dissection of classic developmental problems such as positional memory (Grunwald and Eisen, 2002). Zebrafish fins are relatively simple, nearly symmetric structures composed of several segmented fin rays of intramembranous bone. Each fin ray comprises concave, facing hemirays that surround connective tissue, including fibroblasts and scleroblasts (osteoblasts), and nerves and blood vessels. The process of fin regeneration involves continual, coordinated proliferation and differentiation events. During regenerative growth, new segments are progressively added to the distal end of each ray until the original length of the fin is achieved, usually in about 2 weeks (Akimenko et al., 2003; Poss et al., 2003).

During zebrafish fin regeneration, as in other examples of appendage regeneration, the blastema is the engine for regenerative growth (Tsonis, 1996). Both classic and recent studies have indicated that a signal(s) released by the overlying regeneration epidermis controls or contributes to proliferation of the blastema. Previously, we and others found evidence that signaling by fibroblast growth factors (Fgfs) regulates blastemal proliferation during fin regeneration (Poss et al., 2000; Tawk et al., 2002). The Fgf receptor (Fgfr) subtype *fgfr1* is expressed in pre-blastemal mesenchymal cells during blastema formation, and maintained in subpopulations of blastemal and epidermal cells during outgrowth. *fgf24* (originally called *wfgf*) (Draper et al., 2003), is expressed in the wound epidermis, indicating the presence at least one Fgf during regeneration. In addition, treatment with a pharmacological inhibitor of Fgfrs, SU5402, blocked blastemal proliferation when applied at any stage of regeneration (Poss et al., 2000). Thus, Fgf signaling is a prime candidate for influencing regenerative growth rate in a position-dependent manner.

Here, we show that regenerative growth rate, blastemal proliferation and blastemal length are each highly dependent on the level at which the zebrafish fin is amputated, with greater proximal values than distal. Furthermore, proximal regenerates show higher expression than distal of the Fgf target genes *mkp3* (*dusp6* – Zebrafish Information Network), *sef* (*il17rd* – Zebrafish Information Network) and *spry4*. By way of a new transgenic strain that facilitates specific, inducible blockade of signaling through Fgfrs, we generate an artificial gradient of Fgf signaling that is capable of tightly controlling blastemal proliferation and regenerative rate. Finally, although an extended depletion of Fgf signaling potently inhibits regenerative growth, it does not erase or reprogram the positional information necessary for restoration of correct structures. Our molecular genetic experiments demonstrate that amputation level-specific amounts of Fgf signaling determine position-dependent growth rates in the regenerating vertebrate appendage.

Materials and methods

Zebrafish and surgeries

Zebrafish ~6 months of age of the outbred Ekkwill (EK) strain were used for all fin amputation studies. For single amputation experiments, one-half of the caudal fin was amputated using a razor blade. To obtain double-amputated fins, a cut was first made along the dorsoventral axis 1-2 segments short of the cleft, representing the distal amputation level. Then, the remaining fin tissue was bisected along the PD axis halfway through the remaining fin. Finally, a third cut was made to remove 50% of the remaining ventral lobe tissue. Experimental results were similar when the dorsal lobe was amputated more proximally. After the surgery, animals were returned to recirculating water heated to 26°C or 33°C, a temperature that facilitates faster regeneration than 25-28°C (Johnson and Weston, 1995).

For measurement of regenerative length, two rays (rays 2 and 3 with respect to the most lateral ray; see Fig. 1) from each of the ventral and dorsal portions were measured using Openlab software and the average length between the two rays was recorded. For statistical comparisons, the proximal regenerate lengths were pooled from multiple fish and averaged, to compare with averages of the distal regenerate lengths. To calculate regenerative growth rate, the changes in these averages as time progressed were divided by the time period between measurements.

Analysis of BrdU incorporation and mitosis

A 2.5 mg/ml solution of bromodeoxyuridine (BrdU) in saline was injected intraperitoneally 30 minutes prior to collection. The brief BrdU exposure limits labeling (Nechiporuk and Keating, 2002), an approach that facilitates distinction of highly proliferative areas in immunostained fin regenerates. Staining was performed as described previously (Poss et al., 2002b), using whole double-amputated fins that had been fixed in Carnoy's solution. A rat-derived anti-BrdU monoclonal antibody (Accurate) and a rabbit-derived polyclonal anti-H3P antibody (Upstate Biotechnology) were used for primary antibodies. Laser confocal microscopy (510 LSM, Zeiss) was used to image and analyze 1 μm slices and 10 μm projections of whole-mount samples. The lengths of the BrdU-dense blastemal regions of ventral and dorsal fin rays 2 and 3 were measured with Openlab software, using the middle slice of each projection. The number of H3P-positive cells was counted by hand within an outlined and quantified area (or volume, as it is a projection covering a depth of 10 μm) of BrdU-dense blastemal mesenchyme. Mitoses in proximal regenerate rays 2 and 3, and the corresponding distal rays from each fish were counted and the averages recorded.

In situ hybridization

Whole-mount in situ hybridization was performed on double-amputated fins as described previously (Poss et al., 2000), using digoxigenin-labeled probes for *mkp3*, *sef* and *spry4* (Furthauer et al., 2001; Furthauer, 2002; Tsang et al., 2004). When assaying fin regenerates for graded expression, development of the staining reaction was monitored carefully and stopped immediately after a distinct signal developed in all of the fins (Figs 3, 6 and 8). Cryosectioning of fin regenerates was performed as described previously (Poss et al., 2000).

In experiments where the length of the *mkp3* expression domain was measured (Fig. 4), development of the staining reaction was allowed to progress further, until background staining was detectable. In these fins, *mkp3*-positive areas were measured using Openlab software.

To simultaneously assess *mkp3* expression and BrdU labeling, we cryosectioned fin regenerates (from BrdU-injected animals) that had been stained for *mkp3* expression by whole-mount in situ hybridization. Sections were then stained for BrdU immunoreactivity as described (Poss et al., 2002a).

Construction of *hsp70:dn-fgfr1* animals

A zebrafish *dn-fgfr1* cassette was designed based precisely on the *X. laevis* dominant-negative Fgfr1 (Amaya and Kirschner, 1991), with the tyrosine kinase domain replaced by *egfp*-coding sequence. The

construct is predicted to heterodimerize with all Fgfr subtypes, thereby competitively blocking signaling downstream of all Fgfr subtypes. Briefly, a 3′ truncated fragment of the zebrafish *fgfr1* gene was amplified by PCR using the primers 5′ GTT GAA TTC ATG ATA ATG AAG ACC ACG CTG 3′ and 5′ GTT GGA TCC AGA GCT GTG CAT TTT GGC CAG 3′. This 1.2 kb fragment was directionally cloned into the *Eco*RI/*Bam*HI site of the pEGFP-N3 vector (Clontech). Then, a 2.2 kb *Nhe*I/*Afl*II fragment containing the *fgfr1-egfp* fusion gene was prepared from this plasmid and subcloned behind the 1.5 kb zebrafish *hsp70* promoter (Halloran et al., 2000). Transgenic zebrafish were made by microinjection of the *hsp70:dn-fgfr1* construct using published techniques (Higashijima et al., 1997). Transgenic animals were identified by Egfp fluorescence owing to natural *hsp70* promoter activity in the lens.

Adult heat induction experiments

An electric heater placed in a stand-alone recirculating aquarium unit (Aquatic Habitats) was used for all heat induction experiments. A digital timer automatically activated and deactivated the heater once per day. Water flow adjustment allowed the tuning of peak tank temperatures to 35°C, 36°C, 37°C or 38°C, from a room temperature of 26°C. Exposure to this peak temperature was for about 1 hour, before gradual return to room temperature. To determine effects on Egfp fluorescence, BrdU incorporation or gene expression, a single heat shock was given to animals 5 hours before collecting fins. To detect effects on regenerative growth, animals were maintained in the heat induction unit after amputation and exposed daily to heat induction.

Results

Position-dependent rates of regenerative growth during fin regeneration

To determine to what extent growth rate is dependent on proximodistal (PD) position during zebrafish caudal fin regeneration, we double-amputated caudal fins in a stepwise fashion (Fig. 1A-C) and measured the lengths of the regenerates between 1 and 15 days postamputation (dpa; at 33°C). This surgery allows measurement and comparison of the second- and third-most lateral rays in each lobe, structures that are expected to reach the same length in the completed regenerate (asterisks in Fig. 1A). We found that, as expected, regenerative growth was greater in regenerates that had been more proximally amputated (proximal regenerates; Fig. 1A-D). Statistically significant differences in growth were seen even at the earliest timepoint, 1 dpa. From 3-15 dpa, the ratio of intrafin proximal-to-distal regenerate sizes remained fairly constant, around 1.8. Differences in regenerative growth rates calculated from these measurements peaked at 3 dpa (Fig. 1E). Thus, the regenerating zebrafish fin, like the urodele limb, assigns growth rates based on amputation level.

Position-dependent indices of blastemal length and proliferation during fin regeneration

Intuitively, regenerative growth rate is expected to be highly dependent on blastemal proliferation. During fin regeneration, there is a much greater amount of mesenchymal proliferation than epidermal proliferation, with cycling cells being preferentially localized to the proximal portion of the blastema (Nechiporuk and Keating, 2002; Poss et al., 2002a). We used whole-mount analysis of immunostained, double-amputated fins to assess blastemal morphology and proliferation at 3 dpa, when the regenerative growth rate difference is greatest between proximal and distal regenerates. Thirty minutes prior to collection, animals were injected with BrdU. In confocal slices of whole-mount fins stained for BrdU, we clearly distinguished blastemal mesenchyme with especially high BrdU density (brackets in Fig. 2A,B), versus more proximal, non-blastemal regions with lower BrdU density.

While performing these experiments, we noticed that the length of the blastema appeared greater in proximal regenerates than in distal (Fig. 2A,B). We used digital imaging and computer-assisted measurements to compare this length between proximal and distal rays 2 and 3. We found that the average blastemal length of proximal regenerates from many

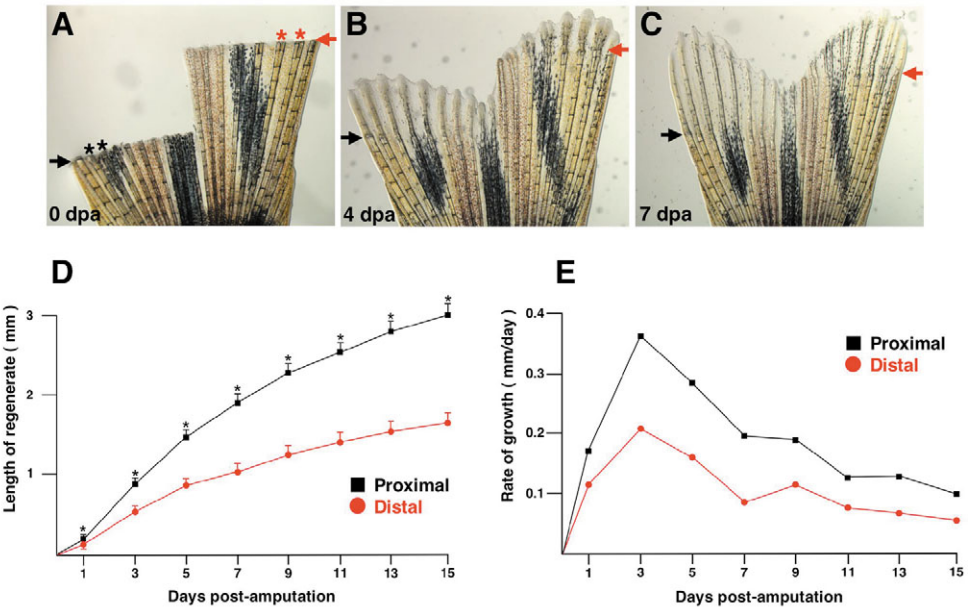

Fig. 1. Amputated zebrafish caudal fins display position-dependent rates of regenerative growth. (A) Appearance of the zebrafish fin immediately following a double amputation surgery, with the injured portion at the top of the image. The amputation planes are indicated by arrows (black, proximal; red, distal), and asterisks mark lateral rays 2 and 3 that are compared in this study. (B) Only 4 days after amputation (dpa; assessed at 33°C), the fin has regenerated a significant number of lost structures. The ventral lobe of the fin (left), after a more proximal amputation, is regenerating more rapidly than the right, dorsal lobe. (C) By 7 dpa, the ventral regenerate has reached nearly the same PD level as the dorsal regenerate. (D) Growth is greater after proximal amputations compared with distal amputations throughout regeneration (mean±s.e.m.; **P*<0.05, *t*-test). (E) Growth rate is greater after proximal amputations than distal throughout regeneration.

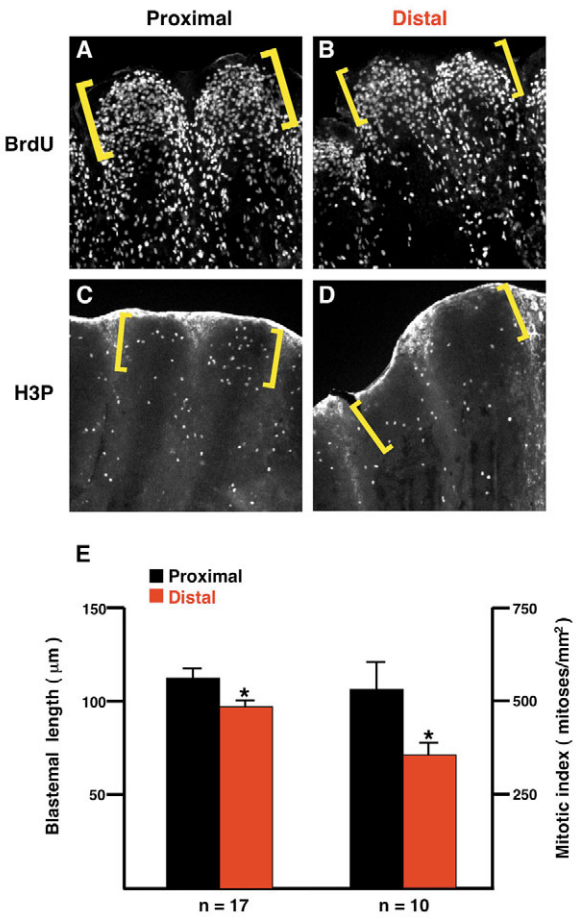

Fig. 2. Blastemal length and mitotic index depend on PD position. (A,B) Proximal and distal 3 dpa regenerates (33°C) of the same fin stained for BrdU incorporation (fins collected 30 minutes post-injection). The proximal regenerate has a greater PD length of especially BrdU-dense blastemal mesenchyme (brackets). (C,D) Proximal and distal 3 dpa regenerates of the same fin stained for phosphorylated Histone-3 (H3P), an indicator of mitosis. Fine points indicate individual mesenchymal mitotic nuclei. This particular fin was chosen because even though it has similar blastemal sizes for the proximal and distal regenerates (brackets; actual BrdU stain is not shown), there are clearly more H3P-positive cells in the proximal blastema. As reported previously, fins show non-specific epidermal fluorescence at the distal edge of the regenerate (Poss et al., 2002b). (E) Quantification of blastemal length and mitotic index at 3 dpa (*P<0.05, t-test).

fish was 113±5 μm (mean ± s.e.m.), compared with 97±3 μm for the distal, a proximal:distal ratio of 1.16 (Fig. 2E; n=17; t-test: P<0.05). We also compared blastemal length within the same fin to control for interfish differences and found that the average proximal:distal length ratio was 1.18±0.07. We then used an antibody against phosphorylated histone-3 (H3P) to count the number of mitoses within BrdU-dense, blastemal mesenchyme in double-amputated fins (Fig. 2C,D). Proximal regenerate blastemas had an average of 535±73 H3P-positive cells/mm^2, versus 356±35 for distal regenerate blastemas, a proximal:distal ratio of 1.50 (Fig. 2E; n=10; t-test: P<0.05;). In intrafin proximal-to-distal comparisons, the average proximal:distal ratio for blastemal mitoses was 1.58±0.23. Thus, position-dependent differences in regenerative growth rates are likely to reflect differences in blastemal length and mitotic index.

Position-dependent properties of Fgf signaling activity during fin regeneration

Pharmacological studies have indicated a requirement for Fgf signaling during fin regeneration (Poss et al., 2000). Therefore, we suspected that differential regulation of Fgf signaling among proximal and distal regenerates might underlie position-dependent blastemal properties and regenerative rate. To identify accurate readouts of Fgf signaling during fin regeneration, we assayed downstream transcriptional targets of Fgf receptor activation. *map kinase phosphatase 3* (*mkp3*), *sef* and *sprouty4* (*spry4*), are each transcriptionally activated by Fgf application in developmental systems, and participate in a negative feedback loop that attenuates the transduced signal (Furthauer et al., 2001; Furthauer et al., 2002; Eblaghie et al., 2003; Kawakami et al., 2003; Tsang et al., 2003). Each of these gene products negatively regulates extra4ellular signal-regulated protein kinase (Erk) activation, with Mkp3 directly dephosphorylating Erk (Tsang and Dawid, 2004). All three genes were induced in both the distal blastema and the basal epidermal layer of the fin regenerate by 3 dpa, mimicking *fgfr1* expression (Fig. 3A) (Poss et al., 2000). Furthermore, as described later, their mRNA expression in these domains is dependent on Fgfr activation. Thus, *mkp3*, *sef* and *spry4* expression report Fgfr signaling in the regenerating zebrafish fin.

To test whether amputation level determines the amount of Fgf signaling, we examined expression of *mkp3*, *sef* and *spry4* in double-amputated fins (Fig. 3B). By carefully monitoring the in situ hybridization reaction, we found that the majority of fins displayed a clearly higher expression level in proximal regenerates versus distal for each gene (*mkp3*, 15 out of 24 fins; *sef*, 8 out of 11; *spry4*, 12 of 18). No fins displayed a higher level of gene expression in distal regenerates. These results indicate that each PD position is assigned a different amount of Fgf signaling after amputation.

In addition, we used target gene expression to assess the domain of active Fgf signaling in proximal and distal regenerates. After fully developing in situ hybridization reactions (see Materials and methods), we observed distinct differences in how far proximally the *mkp3* signal extended in 3 dpa proximal and distal regenerates. In these experiments, we measured the distance from the most distal tip of the *mkp3* expression domain to the most proximal limits. We found that the proximal regenerate expression domain extended 28% further than the distal (Fig. 4A-C; n=8, P<0.005). In intrafin comparisons, the average proximal:distal ratio of this length was 1.31±0.10. Thus, the length of the active Fgf signaling region is determined by amputation level. Interestingly, single-amputated fins stained for both *mkp3* expression and BrdU incorporation (30 minutes exposure) showed very little or no co-labeling in blastemal cells. In other words, the mesenchymal *mkp3* expression domain, likely corresponding to the nonproliferative distal blastema reported by Nechiporuk and Keating (Nechiporuk and Keating, 2002), was located distal to the BrdU-positive proximal blastema (Fig. 4D-F). Instead, BrdU-positive blastemal tissue correlated better with adjacent epidermal *mkp3* expression, suggesting a potential

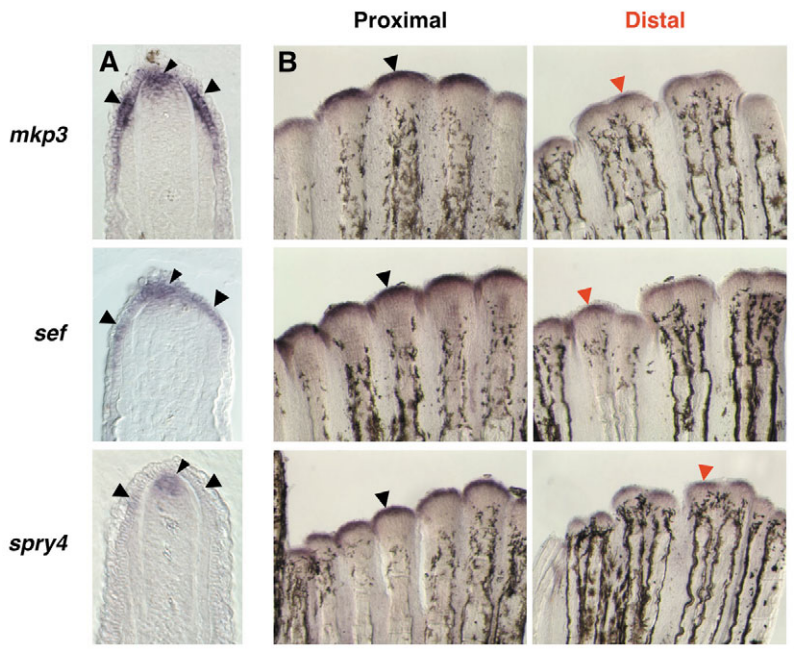

Fig. 3. Amputation level controls the amount of Fgf target gene expression during regeneration. In situ hybridization analysis of Fgf target gene expression in 3 dpa double-amputated fins (33°C). (A) A representative section from a single-amputated fin demonstrates expression for *mkp3*, *sef* and *spry4* in both the basal epidermal layer and the distal region of the blastema (arrowheads indicate in situ hybridization signals). (B) Whole-mount images for each gene show proximal and distal regenerates of the same double-amputated fin. *mkp3* (15 out of 24 regenerates), *sef* (8 out of 11 regenerates) and *spry4* (12 out of 18 regenerates) were usually expressed more strongly in proximal regenerates than distal. We never detected greater expression of these genes in distal regenerates.

paracrine relationship (see Discussion). In summary, our results revealed position-dependent values of regenerative growth rate, blastemal length and mitotic index, and properties of Fgf signaling. In each case, proximal regenerate values were greater than distal regenerate values.

Genetic attenuation of Fgf signaling controls blastemal proliferation and regenerative growth rate

Fgf signaling has been implicated in appendage regeneration in urodeles and zebrafish, mainly by expression assays or through the use of pharmacological inhibitors (Poulin et al., 1993; D'Jamoos et al., 1998; Poss et al., 2000; Yokoyama et al., 2000). In addition, Yokoyama et al. (Yokoyama et al., 2001) showed that application of Fgf10-soaked beads to *X. laevis* tadpole limb stumps could extend the permissive period for regeneration. To define a functional relationship between the amount of Fgf signals, the intensity of blastemal proliferation and regenerative growth rate, we created a transgenic line to permit experimental tuning of Fgf signaling during regeneration. Our molecular genetic strategy is similar to that of Beck et al. (Beck et al., 2003), who made transgenic *X. laevis* to facilitate

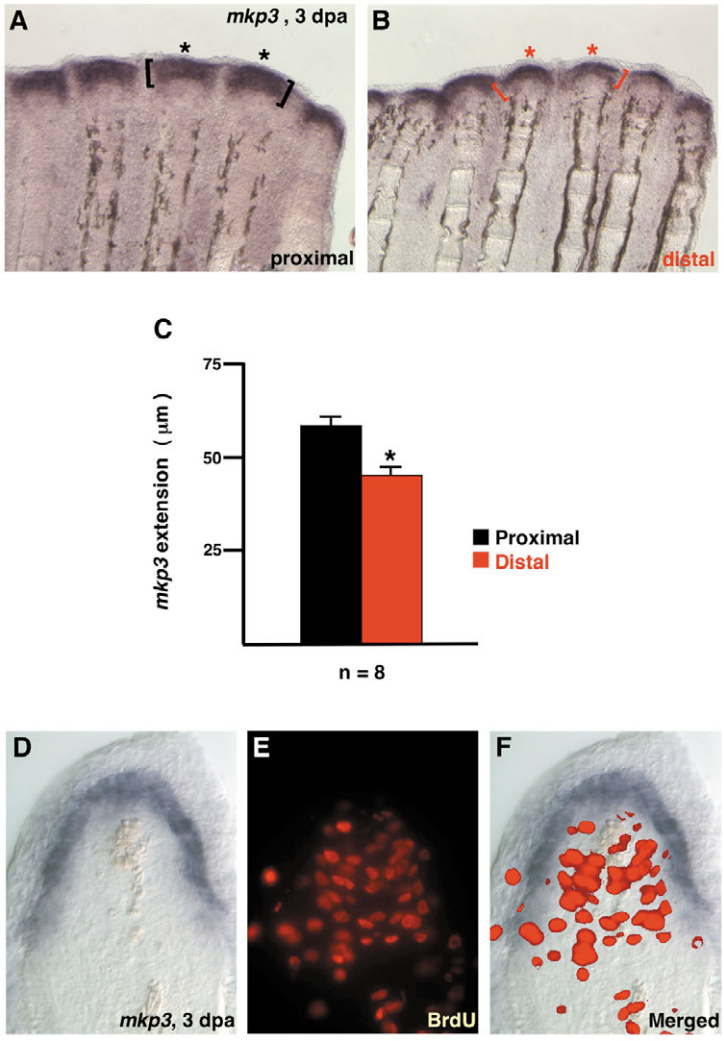

Fig. 4. Position-dependent length of Fgf target gene expression domains. (A,B) Images from the same double-amputated fin regenerate demonstrates a longer PD length of *mkp3* expression (asterisks, brackets) in proximal regenerates. (C) The length of the proximal signal was 28% longer than the distal signal on average (n=8; *P<0.005, t-test). (D-F) 3 dpa fin regenerate (33°C) stained for *mkp3* expression (D) and BrdU incorporation (E). Cells in the distal blastema and basal epidermal layers expressing *mkp3* show little proliferation. However, proliferative blastemal mesenchyme is bordered by epidermal *mkp3* expression/Fgf signaling (F).

inducible modulation of BMP and Notch signaling during tadpole tail regeneration. The [*Tg(hsp70:dn-fgfr1)*^{pd1} strain, referred to hereafter as *hsp70:dn-fgfr1*, harbors a dominant-negative *fgfr1-egfp* fusion gene (*dn-fgfr1*) driven by a heat-inducible zebrafish *hsp70* promoter. We found that this construct had potent inhibitory effects on Fgf signaling. Following a brief heat-shock at the embryo sphere stage (5 hours post-fertilization), *hsp70:dn-fgfr1* animals developed posterior truncations by 24 hpf typical of Fgfr inhibition (Griffin et al., 1995) (Fig. 5A). By assessment of Egfp expression, Dn-fgfr1 was maintained in embryonic tissues at least 24 hours after heat induction (Fig. 5B). Moreover, when adult animals were given a single heat treatment, strong Egfp fluorescence was observed in all cell types of the fin regenerate (Fig. 5C-E).

To test the effect of Dn-fgfr1 induction on fin regeneration, we automated the heat induction protocol so that a single 38°C heat shock would be given daily to adult animals with amputated fins. In these experiments, persistent Dn-fgfr1 expression maintained a robust blockade of fin regeneration (Fig. 5F,G). By contrast, daily heat-induced expression of Egfp via a *hsp70:egfp* strain (Halloran et al., 2000) had no effect on fin regeneration (see Fig. S1 in the supplementary material). Thus, the *hsp70:dn-fgfr1* strain represents a new and important reagent with which to attenuate Fgf signaling during embryogenesis and regeneration.

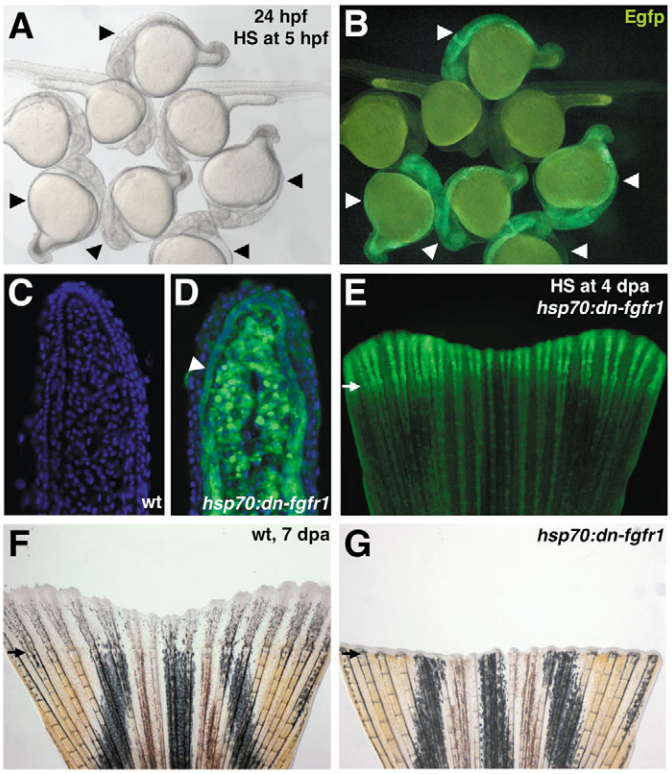

Fig. 5. Transgenic fish that facilitate inducible expression of a dominant-negative Fgfr1 construct. (A,B) *hsp70:dn-fgfr1* transgenic and wild-type embryos were raised until sphere stage at 28°C, shifted to 37°C for 1 hour, and returned to 28°C until 28 hpf. Transgenic embryos are truncated and display Egfp fluorescence (arrowheads). (C,D) Section through a wild-type (C) or *hsp70:dn-fgfr1* (D) 4 dpa fin regenerate 5 hours after heat induction. Strong Egfp fluorescence is observed in all cells of the transgenic regenerate, including the *fgfr1*/*mkp3*/*sef*/*spry4*-positive basal epidermal layer (arrowhead). Nuclei are stained with DAPI (blue). (E) Whole-mount image of fin shown in D, demonstrating Egfp fluorescence throughout the fin. The regenerate shows stronger fluorescence than the non-regenerating portion at 4 dpa. This is probably due in part to the scarceness of pigment cells and differentiated bone in the newly formed tissue that might impede fluorescence detection. (F,G) Adult fin regeneration is blocked by daily heat-induction of *dn-fgfr1* at 38°C. Wild-type (F) and *hsp70:dn-fgfr1* (G) fins are shown at 7 dpa.

We used this strain to establish an experimental range, or gradient, of Fgf signaling during adult zebrafish fin regeneration. First, we created four different heat-induction protocols to apply during regeneration, defined by the peak temperature attained during treatment: 35°C, 36°C, 37°C and 38°C. Experimental control tanks contained transgenic animals maintained at room temperature, or wild-type fish given a 38°C protocol. Visualization of Egfp expression in transgenic fish after a single heat induction showed a clear increase in Dn-Fgfr1 expression with each 1°C increment in temperature (data not shown), indicative of different levels of Fgfr inhibition. To directly test how these conditions affected Fgf signaling, we assayed single-amputated fins for expression of the Fgf target gene *mkp3* 5 hours after heat induction. Control animals displayed normal *mkp3* expression, while 36°C, and more so, 37°C heat induction protocols partially inhibited *mkp3* expression. The 38°C heat shock protocol abolished *mkp3* expression altogether in *hsp70:dn-fgfr1* fin regenerates (Fig. 6A-C). Strong heat shock conditions also attenuated existing *spry4* and *sef* expression, although a longer inhibitory period was required to deplete *sef* expression (data not shown). These results indicated that we could experimentally establish gradations of Fgf signaling similar to physiological amputation level-specific gradations.

To determine how different Fgf signaling amounts impacted blastemal proliferation, we gave *hsp70:dn-fgfr1* fish the same heat-induction protocols and assessed blastemal integrity by BrdU incorporation. We found that blastemal proliferation was affected in a dose-dependent manner by Fgfr inhibition (Fig. 6D-F). A single 36°C or 37°C treatment markedly reduced the number of BrdU-positive cells in the blastema, while the 38°C treatment nearly abolished this structure. Interestingly, only cellular proliferation within the blastema was affected by Fgfr inhibition, while cell populations proximal to the blastema appeared to proliferate normally. Accordingly, we could easily identify an Fgf-dependent proliferative blastemal region that corresponded to an area normally flanked by epidermal Fgf target gene expression (brackets in Fig. 6F).

Next, we applied daily heat inductions to test the effects of this experimental Fgf signaling continuum on regenerative growth rate. We found that regenerative growth rate was also highly sensitive to 1°C temperature increments (Fig. 6G-K). The 37°C incubation slowed regeneration down to about half the rate of uninduced *hsp70:dn-fgfr1* fish at 5 dpa (Fig. 6J,K). Interestingly, 36°C and 37°C regenerates appeared grossly normal, albeit small, with fin ray segments of approximately normal size (Fig. 6H). This observation suggested that rate, and not ray patterning, were the main targets of the inhibition. Our experiments together support the idea that PD disparities in Fgf signaling between proximal and distal regenerates directly translate into different blastemal proliferation and regenerative

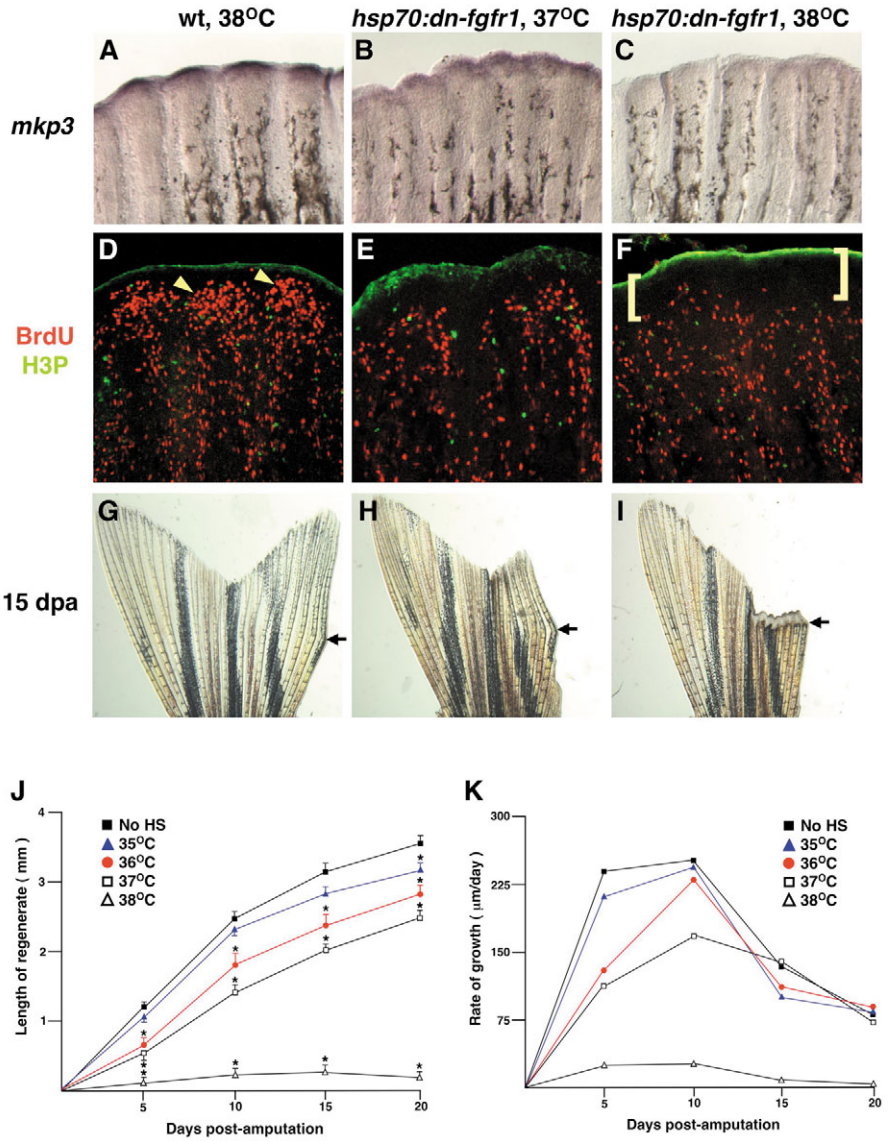

Fig. 6. Experimental attenuation of Fgf signaling alters regenerative proliferation and growth in a dose-dependent manner. (A-C) Images of 4 dpa fin regenerates (26°C) that were heat-induced once at the indicated temperature and collected and examined for *mkp3* expression 5 hours later (violet stain). *mkp3* expression is greatest in wild types treated at 38°C (A), less in *hsp70:dn-fgfr1* transgenics treated at 37°C (B), and undetectable in transgenics given a strong 38°C induction (C). (D-F) Animals treated in the same way as those in A-C, respectively, were assessed for BrdU incorporation and H3P staining. Blastemal BrdU-labeling density (arrowheads in D) is reduced by the 37°C shock in transgenics (E) and still further by the 38°C shock (F). Brackets in (F) indicate a region of Fgf-dependent proliferation. (G-I) Images of 15 dpa fin regenerates given a daily heat induction; to highlight the extent of regeneration, only the right lobe was amputated. Arrows indicate points of amputation. Wild-type fins induced at 38°C or uninduced transgenic fins regenerated normally (G), those induced at 37°C displayed partial regeneration (H), and those induced at 38°C showed a complete block (I). (J,K) Animals were induced daily at four different temperatures, or had no induction, and regenerative growth was measured at 5, 10, 15 and 20 dpa. Regenerative rates were calculated based on these numbers. A daily heat induction to 37°C nearly halves the rate of regeneration at 5 dpa; daily induction to 38°C blocks regeneration (n=5; * P<0.05, significantly different from no HS, t-test).

growth rates. In other words, the amount of Fgf signaling represents an amputation level-specific instruction for position-dependent regenerative growth rates.

A prediction of this model is that a constant level of Fgfr blockade should have greater effects on distal regenerates that contain less Fgf signaling, than on proximal regenerates. To test this prediction, we double-amputated *hsp70:dn-fgfr1* fish and assessed regenerative growth at each amputation level under partial regeneration conditions (36°C) over 12 days. We found that growth of both proximal and distal regenerates was significantly reduced by partial Fgfr inhibition (Fig. 7A). However, whereas the average intrafin P:D length ratio of untreated transgenics at 12 dpa was 1.83±0.06, those heat-shocked at 36°C displayed a 31% higher ratio of 2.39±0.14 (Fig. 7B; n=18 and 21 animals; P<0.001). Thus, growth was slowed to a greater extent in distal regenerates versus proximal. At 4 and 8 dpa (Fig. 7B), the average P:D length ratio was stable (4 dpa, 1.89±0.13; 8 dpa, 1.80±0.08) in untreated fish, while there was a trend towards higher P:D ratios in heat-shocked animals (4 dpa, 2.86±0.52; 8 dpa, 2.95±0.75). Interestingly, we observed a few cases in which distal regeneration was robustly blocked at 4-5 dpa by 36°C treatment despite ongoing proximal regeneration (Fig. 7C-E). These results provide further support that greater amounts of endogenous Fgf signaling are established in proximal regenerates versus distal after amputation, and that these position-dependent Fgf signaling amounts direct regenerative rate.

Positional memory is maintained during Fgfr inhibition

While our experiments demonstrated an intimate relationship between position-dependent Fgf signaling properties and growth rate, we were also curious about whether the Fgf signaling profile represented positional memory in total. That is, does it define both growth rate and the structures to be regenerated?

To examine the validity of this idea, we assessed *mkp3* expression at several timepoints in mid-amputated fins throughout the duration of regeneration (15 dpa). In these

experiments, *mkp3* expression was a robust indicator of PD position. Regenerates displayed a gradual loss of *mkp3* expression intensity, with scarcely detectable marker expression by 15 dpa (Fig. 8A-C). The PD length of the *mkp3* expression domain also decreased gradually during regeneration (Fig. 8D). These initial observations, without functional validation, were consistent with the notion that Fgf signaling properties might indeed encode positional memory.

To functionally test this idea, we artificially depleted Fgf signaling for 30 days after amputation by applying a strong heat shock daily to *hsp70:dn-fgfr1* fish. By blocking Fgf signaling and regeneration for approximately twice the normal duration of fin regeneration, we mimicked the low or absent Fgf signaling normally present at the very end of regeneration (Fig. 8C). To 24 animals that displayed no regeneration after amputation and 30 days of Fgfr inhibition, we then restored Fgf signaling for 15 days by removing heat induction (Fig. 8E-H). Strikingly, 19 of 24 animals showed essentially complete regeneration [11 animals (Fig. 8H)] or patterning defects blocking regeneration of only a small number of rays [8 animals (Fig. 8G)]. Only four out of 24 animals displayed regenerative failure in more than 50% of rays (Fig. 8F); yet, the correct number of structures were regenerated in the unaffected rays. Only one animal of 24 failed to regenerate any rays (Fig. 8E). We deduce from these experiments that Fgf signaling is dispensable for maintaining positional memory. Even if regenerative mechanisms are caged without Fgf signals for 30 days after amputation, stump tissues retain the information necessary to instruct renewal of only those structures lost by injury.

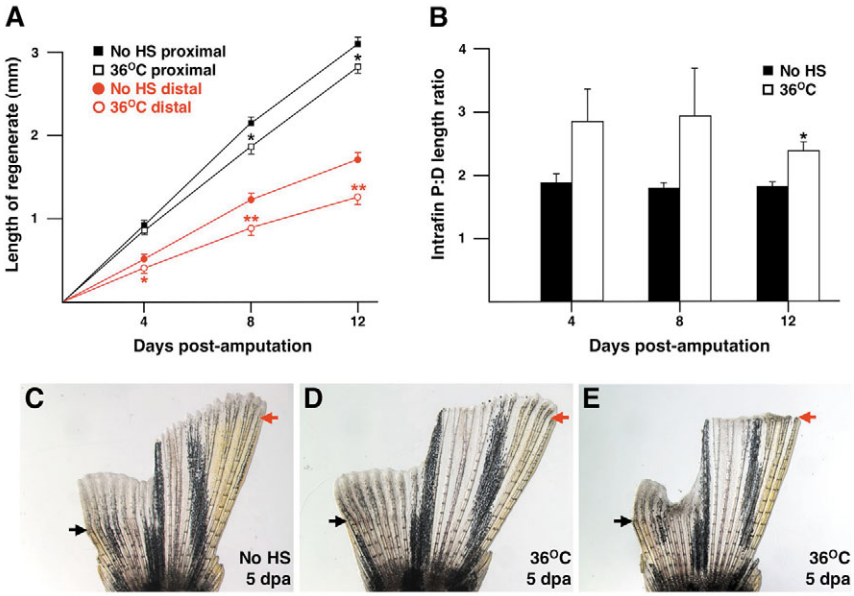

Fig. 7. Regenerative growth in distal fin regenerates is more sensitive to partial Fgfr inhibition than proximal regenerative growth. (A) Daily exposure of double-amputated *hsp70:dn-fgfr1* zebrafish to 36°C heat shock has a significant effect on the growth of proximal and distal fin regenerates. Measurements were averaged from 18 untreated and 21 36°C-treated animals (*P<0.05, significantly different from no HS, t-test: **P<0.001, significantly different from no HS, t-test). (B) Graph of intrafin proximal to distal length ratios using animals described in A. The higher proximal:distal length ratio in 12 dpa 36°C heat-shocked animals indicates a greater sensitivity of distal regenerative growth to partial Fgfr inhibition (*P<0.001, significantly different from no HS, t-test). (C-E) Representative transgenics at 5 dpa given no HS (C) or 36°C heat shocks (D,E). Arrows indicate points of amputation. Some 36°C transgenics appeared similar to untreated transgenics at early timepoints such as 5 dpa (D), while others showed especially poor distal regeneration (E). Such variability is also reflected by the large standard error bars in B that characterize 36°C P:D ratios at 4 and 8 dpa.

Discussion

A model for position-dependent regulation of regenerative growth rate

Here, we have identified molecular and cellular features that distinguish proximal from distal regenerates and explain major position-dependent differences in regenerative growth rate during zebrafish fin regeneration. Our data point to a model for position-dependent control of growth rate mediated by Fgf signaling (Fig. 9A,B).

Amputation of the zebrafish caudal fin stimulates formation of a wound epidermis, blastemal morphogenesis and rapid growth. This growth is dependent on synthesis of Fgfs and signaling through Fgfrs. The more proximal the amputation, the longer the region of active Fgf signaling in epidermal cells. Consequently, more proximally amputated fins establish a greater proximal extension of proliferative blastemal cells adjacent to these epidermal domains. Furthermore, greater amounts of Fgf signaling activity in proximal regenerates translate into higher blastemal mitotic indices. Such position-dependent differences in blastemal function explain position-dependent growth rate, defining Fgf signaling as a graded component of the positional instructions required for accurate regeneration.

While most of our experiments focused on comparison of two amputation levels within a single fin, our data from single-amputated fins support this model. Both amounts and proximal extension of Fgf signaling gradually diminish during regeneration, aligning these parameters with PD position until the process is completed. Such observations explain the gradual decrease in regenerative growth rate from 3 to 15 dpa (Fig. 1). They also indicate that there is not only a mechanism to establish a position-dependent amount of Fgf signaling after amputation, but an additional related mechanism for gradual position-dependent reduction in these amounts to slow and then stop regeneration as it concludes.

Our data suggest that the effect of Fgfr activation on blastemal cells is cell non-autonomous; i.e. Fgf signal transduction in basal epidermal cells somehow influences nearby blastemal cells. Because the Erk signaling inhibitors *mkp3*, *sef* and *spry4* are induced in epidermal cells and are Fgf dependent during fin regeneration, we suspect that Fgfrs regulate blastemal function via a mechanism that involves epidermal Erk activation. According to this model, epidermal cells then release a mitogen that diffuses to

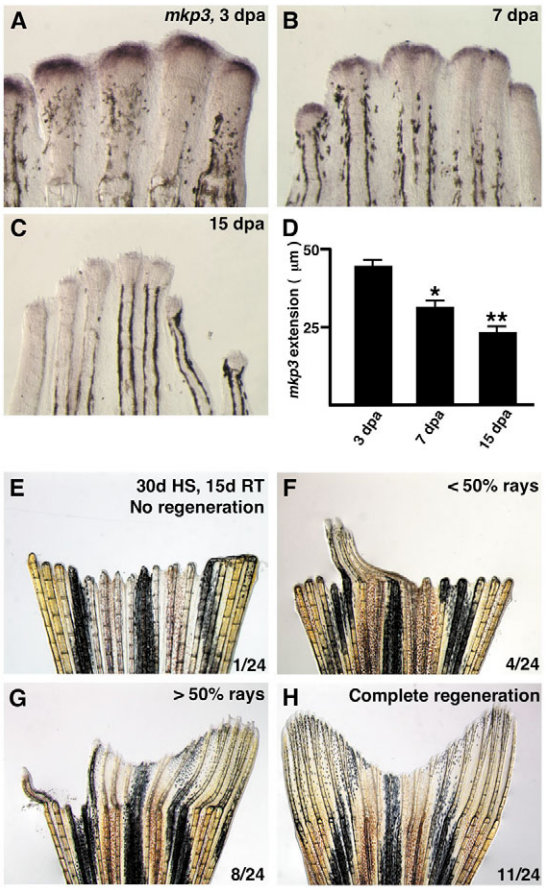

Fig. 8. Positional memory is maintained in the absence of Fgf signaling. (A-C) Expression of *mkp3* assessed by in situ hybridization in 3, 7 and 15 dpa single-amputated fins (33°C). The intensity of *mkp3* expression signal wanes as regeneration progresses. (D) The PD length of the *mkp3* signal is also reduced as regeneration progresses (n=10; **P*<0.001, significantly different from 3 dpa, *t*-test; ***P*<0.005, significantly different from 3 and 7 dpa, *t*-test). (E-H) To test whether a long-term block of Fgf signaling could alter positional memory, 24 *hsp70:dn-fgfr1* fins were amputated and exposed to 30 days of heat induction, followed by 15 days of room temperature treatment. Regeneration was fully blocked during the 30-day period. One of 24 animals showed no recovery after 15 days of restored Fgf signaling (E), while a small number (4/24) had regenerative blocks affecting more than half of the rays (F). The majority of regenerates displayed normal regeneration of more than half of rays (8/24, G) or all rays (11/24, H).

adjacent blastemal cells (Fig. 9B). Sonic hedgehog (*shh*) is a candidate for this mitogen, as it is expressed in basal epidermal cells and its transcription is dependent on Fgfr activation (Laforrest et al., 1998; Poss et al., 2000). Furthermore, cyclopamine, the pharmacological inhibitor of Hedgehog signal transduction, was recently shown to block blastemal proliferation in the regenerating zebrafish fin, as well as the amputated axolotl tail (Quint et al., 2002; Schnapp et al., 2005). Continued candidate approaches should help resolve the downstream mechanisms by which Fgfs modulate blastemal function.

Positional memory

How does position determine Fgf signaling properties in injured tissue? Interestingly, fin cells support faithful regeneration even after many successive amputations. In addition, cultured fin cells act immortal in culture and can be passaged for years (Paw and Zon, 1999). These findings suggest that positional information is quickly set after injury and not based on pre-injury, position-dependent limitations of fin cells with respect to how much and how fast to regenerate. In our experiments, we detected PD differences in growth rate as early as 1 dpa, indicating that instructions for growth rate are followed even as the blastema forms.

It is reasonable to suspect that an Fgf ligand gradient is responsible for the Fgf signaling gradient described in our experiments. We have not been able to conclusively detect position-dependent regulation of *fgf24* mRNA levels (Y.L. and K.D.P., unpublished), but there are many Fgf genes to be examined for position-dependent regulation at the RNA or protein level during fin regeneration. Whatever the primary rate-determinant in the Fgf signaling pathway may be, our data indicate that Fgf signaling translates position into rate, but lies downstream of the master regulator(s) that furnishes position-

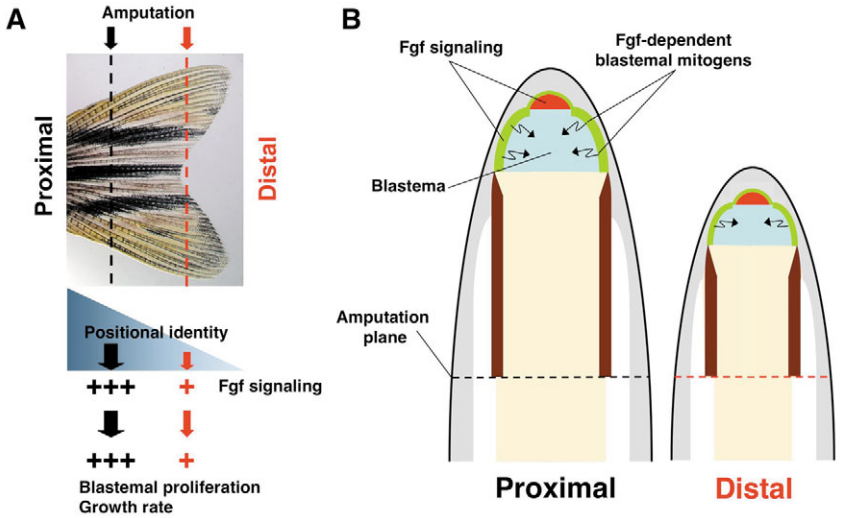

Fig. 9. A model for position-dependent regulation of regenerative growth rate. (A) After amputation, yet undetermined signals recognize position and establish cellular identity. These signals are thought to be present in a gradient along the PD axis, and introduce position-dependent properties of Fgf signaling. (B) The amount and PD length of Fgf signaling, each of which are greater in proximal regenerates, determine the PD length and the mitotic index of adjacent blastemal mesenchyme (blue). Because there is little overlap between highly proliferative blastemal tissue, regions of active Fgf signaling in the epidermis (green) and the distal region of the blastema (red), it is likely that an Fgf-dependent epidermal mitogen mediates blastemal proliferation (arrows). Greater influences by Fgf signaling on blastemal cells of proximal regenerates lead to higher growth rates than distal regenerates.

dependent instructions (Fig. 9A). Removal of Fgf signaling for an extended period does not irreversibly change positional values, while disruption of more upstream factors that regulate the positional memory program is predicted to do so. However, it is tempting to speculate that experimental increases in Fgf signaling levels during later stages of fin regeneration might have the effect of extending the length of the final regenerate.

Two molecules to date have been implicated in maintenance of positional identity during amphibian limb regeneration. Treatment of a wrist level axolotl blastema with retinoic acid (RA) stimulates regeneration of more proximal structures (Maden, 1982; Crawford and Stocum, 1988). Furthermore, direct measurements of RA in limb regenerates indicate a blastemal gradient, with higher RA levels in more proximal blastemas when compared with distal (Scadding and Maden, 1994). These findings indicate that RA levels are important in determining position in blastemal cells, possibly through regulation of Meis genes as reported by Mercader et al. (Mercader et al., 2005) in analysis of axolotl limb regeneration. In the regenerating zebrafish fin, RA treatment can lead to ray fusion, distalizing the bifurcation point of fin rays (White et al., 1994; Laforrest et al., 1998). This result suggests that fin regenerates might be proximalized to some extent by RA, although the idea that RA modulates positional memory in the zebrafish fin requires further experimental testing. Interestingly, RA and Fgf signaling have recently been shown to interact in multiple developing systems (Shiotsugu et al., 2004; Moreno and Kintner, 2004). Thus, it is possible that RA levels assist in establishing regenerative growth rate through the adjustment of Fgf signaling amounts.

The second molecule implicated in positional memory is CD59, a membrane-localized protein whose expression is graded along the PD axis and regulated by RA in the amphibian limb. When CD59 function is blocked in blastemal explant cultures, proximal blastemal behavior – engulfment of distal blastemal explants – is inhibited (da Silva et al., 2002). Furthermore, CD59 overexpression in electroporated axolotl limb regenerates appears to proximalize blastemal cells (Echeverri and Tanaka, 2005). The mechanism by which CD59 might control positional memory remains unclear. Therefore, it would be interesting to functionally examine CD59 during zebrafish fin regeneration as carried out here for Fgf signaling. Moreover, unbiased genetic screens for defects during fin regeneration are possible in zebrafish (Johnson and Weston, 1995; Poss et al., 2002b; Nechiporuk et al., 2003), and can be modified to identify mutants that regenerate too few or too many structures. Such approaches represent an attractive method for increasing the molecular resolution of mechanisms by which positional memory directs appendage regeneration.

We are grateful to M. Keating for generous support while creating transgenic fish. We thank A. Lepilina and A. Henry for excellent animal care, M. Tsang for in situ probes, T. Oliver for help with imaging, and B. Hogan, A. Nechiporuk, S. Odelberg, R. Roberts and V. Yin for helpful comments on the manuscript. Y.L. is a predoctoral fellow of the American Heart Association. This work was supported by a grant from the Whitehead Foundation to K.D.P.

References

Akimenko, M. A., Mari-Beffa, M., Becerra, J. and Geraudie, J. (2003). Old questions, new tools, and some answers to the mystery of fin regeneration. *Dev. Dyn.* **226**, 190-201.

Amaya, E., Musci, T. J. and Kirschner, M. W. (1991). Expression of a dominant negative mutant of the FGF receptor disrupts mesoderm formation in Xenopus embryos. *Cell* **66**, 257-270.

Beck, C. W., Christen, B. and Slack, J. M. (2003). Molecular pathways needed for regeneration of spinal cord and muscle in a vertebrate. *Dev. Cell* **5**, 429-439.

Becker, C. G., Lieberoth, B. C., Morellini, F., Feldner, J., Becker, T. and Schachner, M. (2004). L1.1 is involved in spinal cord regeneration in adult zebrafish. *J. Neurosci.* **24**, 7837-7842.

Crawford, K. and Stocum, D. L. (1988). Retinoic acid proximalizes level-specific properties responsible for intercalary regeneration in axolotl limbs. *Development* **104**, 703-712.

da Silva, S. M., Gates, P. B. and Brockes, J. P. (2002). The newt ortholog of CD59 is implicated in proximodistal identity during amphibian limb regeneration. *Dev. Cell* **3**, 547-555.

D'Jamoos, C. A., McMahon, G. and Tsonis, P. A. (1998). Fibroblast growth factor receptors regulate the ability for hindlimb regeneration in Xenopus laevis. *Wound Repair Regen.* **6**, 388-397.

Draper, B. W., Stock, D. W. and Kimmel, C. B. (2003). Zebrafish fgf24 functions with fgf8 to promote posterior mesodermal development. *Development* **130**, 4639-4654.

Eblaghie, M. C., Lunn, J. S., Dickinson, R. J., Munsterberg, A. E., Sanz-Ezquerro, J. J., Farrell, E. R., Mathers, J., Keyse, S. M., Storey, K. and Tickle, C. (2003). Negative feedback regulation of FGF signaling levels by Pyst1/MKP3 in chick embryos. *Curr. Biol.* **13**, 1009-1018.

Echeverri, K. and Tanaka, E. M. (2005). Proximodistal patterning during limb regeneration. *Dev. Biol.* **279**, 391-401.

Furthauer, M., Reifers, F., Brand, M., Thisse, B. and Thisse, C. (2001). sprouty4 acts in vivo as a feedback-induced antagonist of FGF signaling in zebrafish. *Development* **128**, 2175-2186.

Furthauer, M., Lin, W., Ang, S. L., Thisse, B. and Thisse, C. (2002). Sef is a feedback-induced antagonist of Ras/MAPK-mediated FGF signalling. *Nat. Cell Biol.* **4**, 170-174.

Goodwin, P. A. (1946). A comparison of regeneration rates and metamorphosis in Triturus and Amblystoma. *Growth* **10**, 75-87.

Griffin, K., Patient, R. and Holder, N. (1995). Analysis of FGF function in normal and no tail zebrafish embryos reveals separate mechanisms for formation of the trunk and the tail. *Development* **121**, 2983-2994.

Grunwald, D. J. and Eisen, J. S. (2002). Headwaters of the zebrafish – emergence of a new model vertebrate. *Nat. Rev. Genet.* **3**, 717-724.

Halloran, M. C., Sato-Maeda, M., Warren, J. T., Su, F., Lele, Z., Krone, P. H., Kuwada, J. Y. and Shoji, W. (2000). Laser-induced gene expression in specific cells of transgenic zebrafish. *Development* **127**, 1953-1960.

Higashijima, S., Okamoto, H., Ueno, N., Hotta, Y. and Eguchi, G. (1997). High-frequency generation of transgenic zebrafish which reliably express GFP in whole muscles or the whole body by using promoters of zebrafish origin. *Dev. Biol.* **192**, 289-299.

Iten, L. E. and Bryant, S. V. (1976). Regeneration from different levels along the tail of the newt, Notophthalmus viridescens. *J. Exp. Zool.* **196**, 293-306.

Johnson, S. L. and Weston, J. A. (1995). Temperature-sensitive mutations that cause stage-specific defects in Zebrafish fin regeneration. *Genetics* **141**, 1583-1595.

Kawakami, Y., Rodriguez-Leon, J., Koth, C. M., Buscher, D., Itoh, T., Raya, A., Ng, J. K., Esteban, C. R., Takahashi, S., Henrique, D. et al. (2003). MKP3 mediates the cellular response to FGF8 signalling in the vertebrate limb. *Nat. Cell Biol.* **5**, 513-519.

Laforest, L., Brown, C. W., Poleo, G., Geraudie, J., Tada, M., Ekker, M. and Akimenko, M. A. (1998). Involvement of the sonic hedgehog, patched 1 and bmp2 genes in patterning of the zebrafish dermal fin rays. *Development* **125**, 4175-4184.

Maden, M. (1976). Blastemal kinetics and pattern formation during amphibian limb regeneration. *J. Embryol. Exp. Morphol.* **36**, 561-574.

Maden, M. (1982). Vitamin A and pattern formation in the regenerating limb. *Nature* **295**, 672-675.

Mercader, N., Tanaka, E. M. and Torres, M. (2005). Proximodistal identity during vertebrate limb regeneration is regulated by Meis homeodomain proteins. *Development* **132,** 4131-4142.

Moreno, T. A. and Kintner, C. (2004). Regulation of segmental patterning by retinoic acid signaling during Xenopus somitogenesis. *Dev. Cell* **6,** 205-218.

Morgan, T. H. (1906). The physiology of regeneration. *J. Exp. Zool.* **3,** 457-503.

Nechiporuk, A. and Keating, M. T. (2002). A proliferation gradient between proximal and msxb-expressing distal blastema directs zebrafish fin regeneration. *Development* **129**, 2607-2617.

Nechiporuk, A., Poss, K. D., Johnson, S. L. and Keating, M. T. (2003). Positional cloning of a temperature-sensitive mutant emmental reveals a role for sly1 during cell proliferation in zebrafish fin regeneration. *Dev. Biol.* **258**, 291-306.

Paw, B. H. and Zon, L. I. (1999). Primary fibroblast cell culture. *Methods Cell Biol.* **59**, 39-43.

Poss, K. D., Shen, J., Nechiporuk, A., McMahon, G., Thisse, B., Thisse, C. and Keating, M. T. (2000). Roles for Fgf signaling during zebrafish fin regeneration. *Dev. Biol.* **222**, 347-358.

Poss, K. D., Wilson, L. G. and Keating, M. T. (2002a). Heart regeneration in zebrafish. *Science* **298**, 2188-2190.

Poss, K. D., Nechiporuk, A., Hillam, A. M., Johnson, S. L. and Keating, M. T. (2002b). Mps1 defines a proximal blastemal proliferative compartment essential for zebrafish fin regeneration. *Development* **129**, 5141-5149.

Poss, K. D., Keating, M. T. and Nechiporuk, A. (2003). Tales of regeneration in zebrafish. *Dev. Dyn.* **226**, 202-210.

Poulin, M. L., Patrie, K. M., Botelho, M. J., Tassava, R. A. and Chiu, I. M. (1993). Heterogeneity in the expression of fibroblast growth factor receptors during limb regeneration in newts (Notophthalmus viridescens). *Development* **119**, 353-361.

Quint, E., Smith, A., Avaron, F., Laforest, L., Miles, J., Gaffield, W. and Akimenko, M. A. (2002). Bone patterning is altered in the regenerating zebrafish caudal fin after ectopic expression of sonic hedgehog and bmp2b or exposure to cyclopamine. *Proc. Natl. Acad. Sci. USA* **99**, 8713-8718.

Raya, A., Koth, C. M., Buscher, D., Kawakami, Y., Itoh, T., Raya, R. M., Sternik, G., Tsai, H. J., Rodriguez-Esteban, C. and Izpisua-Belmonte, J. C. (2003). Activation of Notch signaling pathway precedes heart regeneration in zebrafish. *Proc. Natl. Acad. Sci. USA* **100**, 11889-11895.

Scadding, S. R. and Maden, M. (1994). Retinoic acid gradients during limb regeneration. *Dev. Biol.* **162**, 608-617.

Schnapp, E., Kragl, M., Rubin, L. and Tanaka, E. M. (2005). Hedgehog signaling controls dorsoventral patterning, blastema cell proliferation and cartilage induction during axolotl tail regeneration. *Development* **132**, 3243-3253.

Shiotsugu, J., Katsuyama, Y., Arima, K., Baxter, A., Koide, T., Song, J., Chandraratna, R. A. and Blumberg, B. (2004). Multiple points of interaction between retinoic acid and FGF signaling during embryonic axis formation. *Development* **131**, 2653-2667.

Spallanzani, A. (1769). An essary on animal reproductions. (Trans. M. Maty) London: T. Becket.

Tassava, R. A. and Goss, R. J. (1966). Regeneration rate and amputation level in fish fins and lizard tails. *Growth* **30**, 9-21.

Tawk, M., Tuil, D., Torrente, Y., Vriz, S. and Paulin, D. (2002). High-efficiency gene transfer into adult fish: a new tool to study fin regeneration. *Genesis* **32**, 27-31.

Tsang, M. and Dawid, I. B. (2004). Promotion and attenuation of FGF signaling through the Ras-MAPK pathway. *Sci. STKE* **2004**, pe17.

Tsang, M., Maegawa, S., Kiang, A., Habas, R., Weinberg, E. and Dawid, I. B. (2004). A role for MKP3 in axial patterning of the zebrafish embryo. *Development* **131**, 2769-2779.

Tsonis, P. A. (1996). *Limb Regeneration*. Cambridge: Cambridge University Press.

White, J. A., Boffa, M. B., Jones, B. and Petkovich, M. (1994). A zebrafish retinoic acid receptor expressed in the regenerating caudal fin. *Development* **120**, 1861-1872.

Yokoyama, H., Yonei-Tamura, S., Endo, T., Izpisua Belmonte, J. C., Tamura, K. and Ide, H. (2000). Mesenchyme with fgf-10 expression is responsible for regenerative capacity in *Xenopus* limb buds. *Dev. Biol.* **219**, 18-29.

Yokoyama, H., Ide, H. and Tamura, K. (2001). FGF-10 stimulates limb regeneration ability in *Xenopus laevis*. *Dev. Biol.* **233**, 72-79.